Scilight

Journal of Mechanical Engineering and Manufacturing
https://www.sciltp.com/journals/jmem

Article

A Comprehensive Evaluation of Peel and Tensile Strength in Adhesive Bonding

André F. V. Pedroso [1,2,*], Raul D. S. G. Campilho [1,3], Arnaldo G. Pinto [1], Paulo J. R. O. Nóvoa [1,3], José G. F. Barbosa [1] and Diogo A. M. Solha [1]

[1] CIDEM, ISEP, Polytechnic of Porto, Rua Dr. António Bernardino de Almeida, 4249-015 Porto, Portugal
[2] Faculty of Engineering, University of Porto, Department of Mechanical Engineering, Rua Dr Roberto Frias, 400, 4200-465 Porto, Portugal
[3] Associate Laboratory for Energy, Transports and Aerospace (LAETA-INEGI), Rua Dr Roberto Frias, 400, 4200-465 Porto, Portugal
* Correspondence: afvpe@isep.ipp.pt; Tel.: +351-228340500

How To Cite: Pedroso, A.F.V.; Campilho, R.D.S.G.; Pinto, A.G.; et al. A Comprehensive Evaluation of Peel and Tensile Strength in Adhesive Bonding. *Journal of Mechanical Engineering and Manufacturing* **2026**. https://doi.org/10.53941/jmem.2026.100018

Received: 25 January 2026
Revised: 21 February 2026
Accepted: 3 March 2026
Published: 24 April 2026

Abstract: Adhesive bonding has become a key joining technique in structural engineering; however, accurate mechanical characterization of adhesive joints strongly depends on reliable testing methodologies. Despite the widespread use of peel and tensile tests, limited studies report the validation of dedicated fixtures capable of consistently assessing adhesives with markedly different mechanical behaviors. This work presents the experimental validation of newly developed in-house fixtures for floating roller peel testing (ASTM D 3167) and tensile butt-joint testing (ASTM D 2095). The devices were evaluated using two epoxy adhesives (Araldite® AV 138 and Araldite® 420 A/B) and one polyurethane adhesive (SikaForce® 710). Results showed that grit blasting significantly enhanced peel strength, particularly for epoxy adhesives. SikaForce® 710 exhibited the highest peel strength (up to 5.41 N/mm), while Araldite® AV 138 demonstrated the highest tensile strength (29.04 MPa), closely matching manufacturer data. A clear contrast between ductility-driven peel performance and intrinsic tensile strength was observed. Predominantly cohesive failure in tensile tests confirmed effective adhesion to stainless steel substrates. The developed fixtures demonstrated robustness, repeatability, and suitability for characterizing adhesives across a wide range of stiffness and ductility, providing practical guidance for adhesive selection and joint design in structural applications.

Keywords: adhesive bonding; floating roller peel test; tensile butt-joints test; mechanical properties of adhesives; failure modes

1. Introduction

Adhesive bonding has emerged as a critical joining technique in the automotive, aerospace, and construction industries due to its unique capability to form strong and durable connections between dissimilar materials [1]. Unlike traditional mechanical fasteners or welding methods [2], adhesive bonding allows for a more uniform distribution of stresses across the joint, which can reduce stress concentrations and improve fatigue resistance [3]. Furthermore, this joining method enables the assembly of lightweight structures without compromising structural integrity, supports the bonding of complex geometries, and can enhance corrosion resistance by eliminating the need for holes or other disruptive mechanical connections. As a result, adhesive bonding has become increasingly indispensable in applications where performance, reliability, and weight reduction are critical design criteria [4,5]. Figure 1 provides an incisive insight into adhesively bonded joints design.

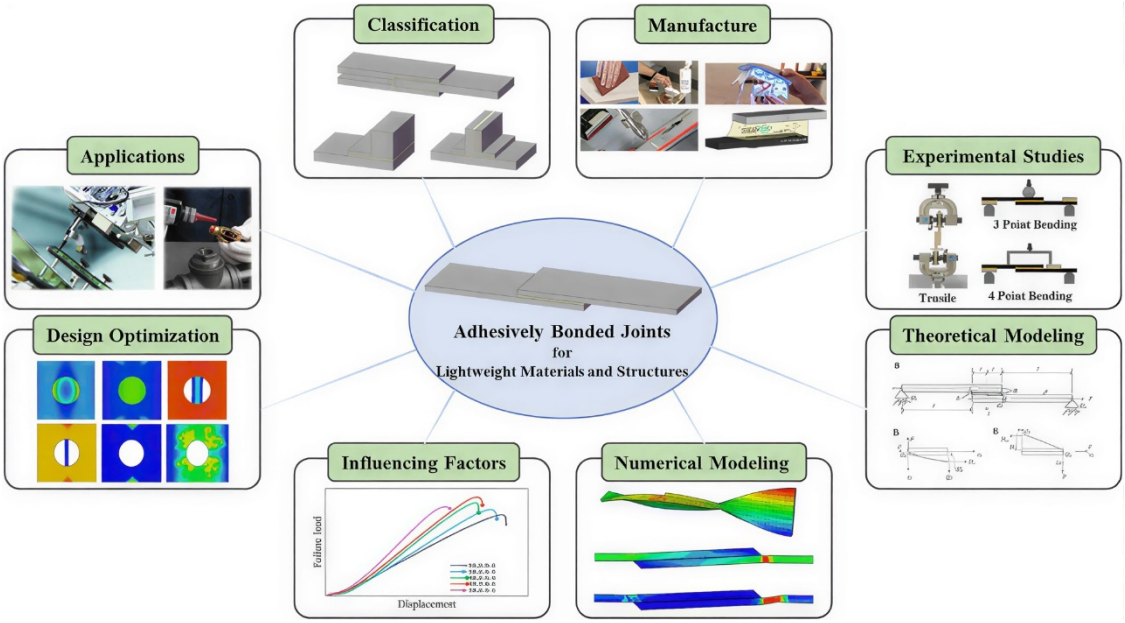

Figure 1. Proposed structure for a state-of-the-art review addressing adhesively bonded joints [4].

Frascio et al. [6] reviewed recent modelling and experimental advances in the design for additive manufacturing of bonded joints, focusing on polymer-based processes. The paper synthesizes tailoring strategies for additively manufactured adherends and adhesives, establishing the state of the art and identifying emerging opportunities from developments in design methodologies, additive processes, and materials. Years later, Borges et al. [7] reviewed the continuous evolution of adhesive bonding, highlighting its expanding industrial relevance driven by composite adoption and dissimilar material joining. Emphasizing advances in adhesive formulation, joint design, manufacturing, and modelling, the review synthesizes recent developments and identifies emerging opportunities for safer, more reliable, and durable adhesive bonding technologies. Karthikeyan and Naveen [8] focused on reviewing adhesive bonding techniques for large-scale composite structures, examining bonding methods, surface treatments, reinforcement strategies, and joint geometries; highlighting shear strength, fracture toughness, fatigue resistance, and vibration behaviour.

This versatility enables the development of lightweight and high-strength structures, which is increasingly important in modern engineering applications where performance, efficiency, and sustainability are critical [9,10]. By allowing the reliable joining of dissimilar materials such as metals, composites, and polymers, adhesive bonding facilitates innovative design solutions that would be difficult or impossible with conventional fastening methods [11]. Moreover, the ability to maintain structural integrity while reducing weight contributes to improved energy efficiency, particularly in automotive [12] and aerospace applications, where lower mass directly translates into reduced fuel consumption and emissions [13–15]. The technique also supports the production of components with complex geometries and thin-walled structures, expanding design freedom while preserving mechanical performance.

Adhesive bonding plays a pivotal role in advanced manufacturing processes for composite [16,17], and metallic components in the aerospace industry as presented by Bañon et al. [18] who offers an overview of adhesive bonding operations for aeronautical materials, examining Aluminium (Al), Titanium (Ti), and composites in aircraft manufacturing [19]. Emphasizing bonding technologies for hybrid structures, the study analyses rigid and tacky adhesives, surface activation methods, and their effects on wettability and adhesion, highlighting surface preparation's critical role in bond durability and reliability. Consequently, adhesive bonding has become an indispensable process in industries that demand a balance of strength, durability, and lightweight construction [20]. As mentioned in the work carried out by Katsiropoulos et al. [21] many types of commercial aircraft benefit considerably from the weight reduction offered by the bonded composite assemblies, as is the case with the AIRBUS A380 (Figure 2).

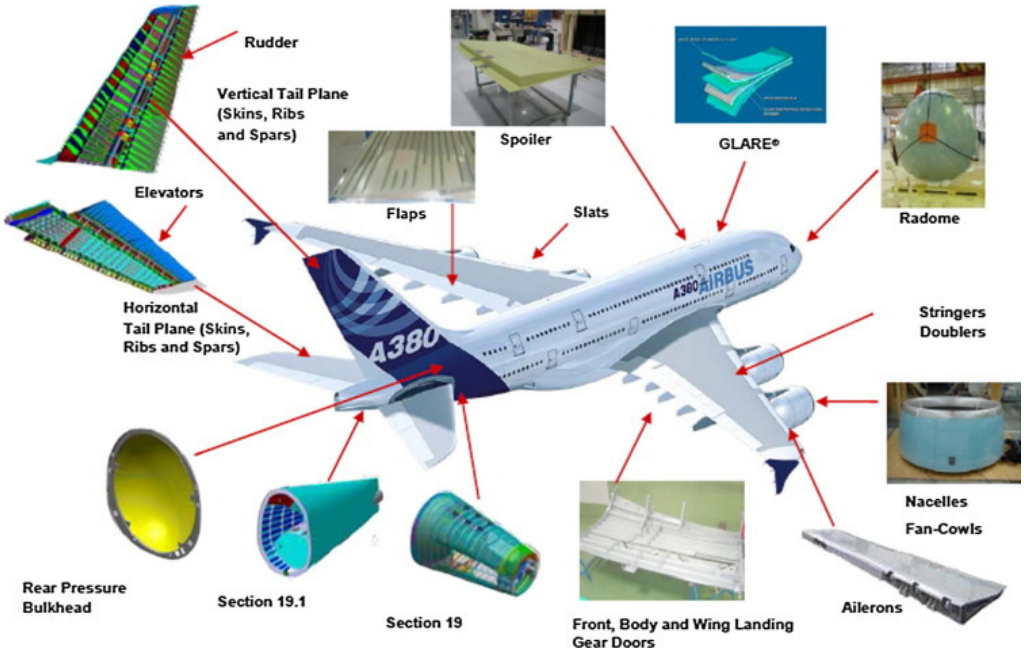

Figure 2. Adhesive bonding applications in the Airbus A380 programme [21].

However, the performance of adhesive joints is highly dependent on a range of factors, including the preparation of the bonding surfaces [22], the selection of the adhesive [23], the curing conditions, and the environmental conditions to which the joint is exposed [24]. Surface preparation is particularly critical, as it governs the wettability, adhesion, and mechanical interlocking between the adhesive and the substrates. Demiral [25] synthesized existing knowledge on the mechanical performance of polymer adhesives under tensile, shear, fracture, fatigue, creep, and impact loading. By combining experimental evidence with computational modelling and contemporary data-driven methodologies, the work contextualizes localized deformation and failure mechanisms within an overarching structure–performance paradigm.

The choice of adhesive influences not only the initial bond strength but also the joint's resistance to mechanical, thermal, and chemical stresses [26]. Curing parameters, such as temperature, time, and pressure, directly impact the adhesive's crosslinking density and mechanical properties. Fan et al. [27] performed systematic evaluations of the bonding performance and tack-free time of epoxy resin adhesives. The findings indicate that, for equivalent curing durations, the tensile bond strength of the epoxy resin–steel interface increases with rising curing temperatures. Additionally, environmental factors, including humidity, temperature fluctuations, and exposure to aggressive chemicals or UV radiation [28], can degrade the adhesive over time, altering the joint's strength and potentially changing its failure mode from cohesive to adhesive. Collectively, these factors underscore the complexity of achieving reliable and durable adhesive joints and highlight the necessity for careful process optimization and quality control in engineering applications [29].

To evaluate the performance and durability of adhesive joints under controlled conditions, mechanical testing methods such as the floating roller peel test and testing of butt-joints in tension are commonly employed [20,30]. The floating roller peel test [31] is particularly suited for assessing the peel strength of flexible adhesive joints, as it provides a consistent and reproducible peeling action that minimizes bending stresses in the substrate. Bartlett et al. [32] presented a comprehensive review of peel mechanics in layered materials, tracing the evolution of peel tests and proposing a unified categorization based on elasticity and debonding behaviour. The study evaluates analytical approaches, material and geometric effects, and highlights implications for advanced applications, including aerospace composites, bio-inspired systems, and structured systems through kirigami and architectural geometries. Pan et al. [33] investigated the influence of Surface Roughness (SR) on the interlaminar strength of Carbon Fibre Reinforced Polymer (CFRP)/Magnesium (Mg) alloy grit-blasted laminates. The findings reveal that increased surface roughness markedly enhances the peel strength. Park et al. [34] also conducted the peel test applied to self-adhesive waterproofing sheets, which are used to caulk onsite concrete, although not being available any standardised methodology to quantify directly the adhesion strength of waterproofing sheets. Bahrami et al. [35] investigated the interlaminar bond strength, flexural behaviour, and hardness of carbon/flax/polyamide hybrid bio-composites, employing floating roller peel test (Figure 3), three-point bending, and macro-hardness tests, respectively.

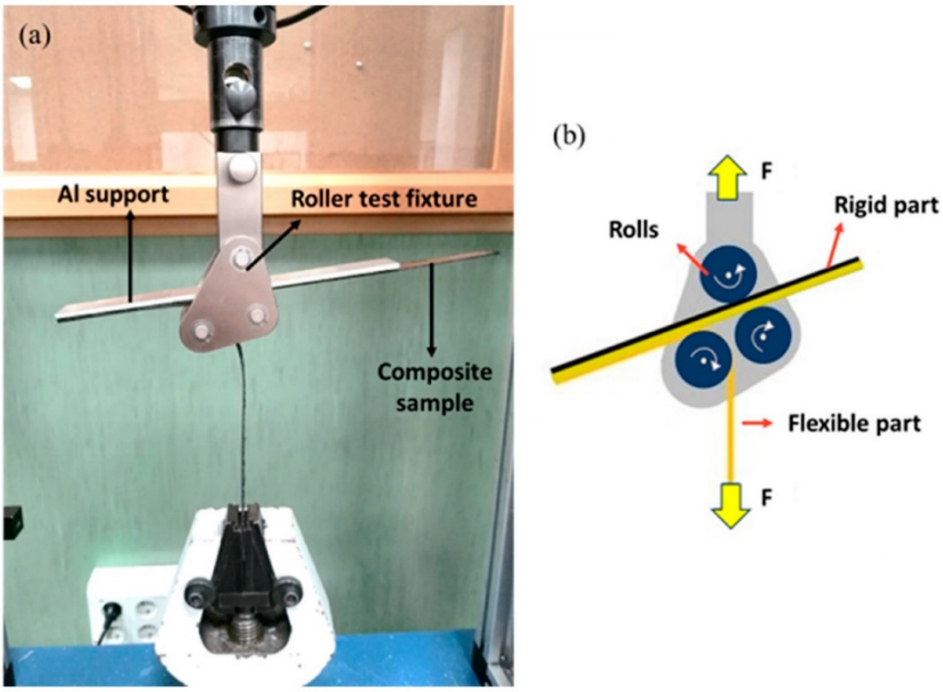

Figure 3. (**a**) Physical configuration of the floating roller peel test, showing the arrangement of components; (**b**) schematic representation of the specimen positioned between the rollers in the floating roller peel test [35].

Tensile testing, in contrast, evaluates the capacity of adhesive joints, including butt joints, to resist forces applied perpendicular to the bonded interface. This approach yields essential data on ultimate tensile strength (σ_u), elongation at failure (ε_u), and the prevailing failure type (adhesive, cohesive, and/or mixed), encompassing both cohesive failure within the adhesive and adhesive failure at the substrate interface. Back in 2007, Öchsner et al. [36] introduced a novel evaluation method for adhesive butt joints, relating the deformation of the adhesive layer–contraction and elongation–to unique values of Young's modulus (E) and Poisson's ratio (v). A numerical parametric study assessed the influence of various adherend and adhesive materials, as well as differing butt-joint geometries, on joint mechanical behaviour. Raffa et al. [37] developed a novel analytical model for thin structural adhesives in tube-to-tube butt joints. The objective was to define an interface condition enabling the effective substitution of the adhesive layer in numerical simulations. The model employs a nonlinear, rate-dependent imperfect interface law, accurately capturing both brittle and ductile stress–strain responses under combined tensile–torsion loading.

This study aims to investigate the peel strength of adhesive joints using the floating roller peel test [38] and butt-joint test [39,40] methods, with particular focus on three widely employed adhesives: Araldite® 420 A/B, Araldite® AV 138 M-1/HV998-1 and SikaForce® 710 L100. The adhesives were bonded to Aluminium (Al) substrates in the first test and were bonded to AISI 304 stainless steel for the second test. The selection relies on their relevance in structural applications and their contrasting mechanical properties [41]. The performance of the adhesive joints was evaluated through a series of carefully designed experimental procedures, including controlled surface preparation, adhesive application, and curing under standardised conditions. The study further considers the influence of key factors such as adhesive thickness (t_A), substrate surface treatment, and test parameters on joint performance.

Despite the extensive body of research on adhesive bonding and mechanical characterisation methods, important aspects remain insufficiently clarified. In particular, the interaction between intrinsic adhesive mechanical properties (stiffness, ductility, and brittleness) and test configuration has not been systematically evaluated within a unified experimental framework. Many existing studies focus either on bulk adhesive properties or on a single joint configuration, without integrating peel and tensile characterisation to distinguish between ductility-driven energy dissipation in peel loading and intrinsic normal tensile strength. Furthermore, limited attention has been given to the experimental validation of custom-designed fixtures capable of ensuring alignment accuracy, controlled adhesive thickness, and repeatable loading conditions across structurally distinct adhesives. These limitations hinder a comprehensive understanding of how adhesive mechanical behaviour, surface preparation, and loading mode jointly influence failure mechanisms and joint performance.

To address this gap, the present study combines floating roller peel tests and tensile butt-joint tests on adhesives with markedly different mechanical characteristics, using controlled specimen geometries and validated alignment fixtures. This integrated approach enables direct comparison between peel performance and tensile strength while ensuring experimental robustness and reproducibility.

In this work, the Section 1 established the theoretical framework underpinning adhesive bonding, providing a detailed overview of the fundamental principles governing adhesion, joint mechanics, and the advantages and limitations of adhesive bonding in industrial applications. Additionally, a comprehensive review of the existing literature situates the current investigation within the broader context of adhesive technology, identifying gaps in knowledge and highlighting the need for systematic evaluation of peel and tensile performance under standardised test methods. Section 2 outlines the experimental methodology employed to evaluate the performance of Araldite® 420 A/B, Araldite® AV 138 M-1/HV998-1 and SikaForce® 710 L100 using the floating roller and butt-joint test methods, including detailed descriptions of substrate preparation, adhesive application, curing conditions, and measurement protocols. Section 3 presents and analyses the experimental results obtained with the three adhesives and for the different conditions used in the floating roller peel tests and the tensile tests with butt joints. Finally, Section 4 concludes the study by highlighting its contributions to bridging the literature gap regarding the application of the floating roller and butt-joint tests to the three adhesives used in this work, emphasizing both methodological insights and practical recommendations for future research and industrial practice.

2. Materials and Testing Procedure

This chapter presents the results of peel tests conducted using the floating roller methodology and tensile tests of butt joints. There are two series of tests within the floating roller method: the first series will comprise specimens to which adherends were abraded with sandpapered, and the second series will include specimens submitted to grit blasting surface preparation.

2.1. Substrates/Adherends

For the floating roller peel tests, the joints consisted of a flexible substrate bonded to a rigid substrate. The flexible substrates, with a thickness (t_S) of 0.5 mm, were fabricated from aluminium AW 1050, while the rigid substrates, with a t_S = 3 mm, were made from Al-alloy AW 6082-T6. The Al-alloy AW 1050 is characterized by low mechanical strength, high corrosion resistance, excellent thermal and electrical conductivity, good formability and weldability, high reflectivity, low polishability, and limited machinability. It is commonly used in pharmaceutical applications, signage, the chemical industry, and similar fields [42].

The Al-alloy AW 6082-T6 is a medium-strength structural alloy belonging to the Al–Mg–Si series, distinguished by its excellent mechanical properties, good corrosion resistance, and favourable machinability. It exhibits a high strength-to-weight ratio, good weldability, and satisfactory surface finish characteristics, making it particularly suitable for load-bearing and precision-engineered components. Owing to these properties, AW 6082-T6 is widely employed in structural applications within the transport, marine, and aerospace industries, as well as in mechanical engineering and architectural frameworks [43].

For the butt-joint test, the substrates are fabricated from AISI 304 stainless steel, which is the best known and most widely used chromium-nickel steels.

2.2. Adhesives

Two epoxy adhesives (Araldite® AV 138 and Araldite® 420 A/B) and one polyurethane adhesive (SikaForce® 710) were employed in the tests.

Araldite® AV 138M-1, combined with hardener HV 998-1, is a two-component thixotropic epoxy system that exhibits a grey colour upon mixing. The adhesive cures at room temperature within 24 h, while curing at 100 °C reduces the time to just 10 min. It is characterized by high stiffness and mechanical strength but low ductility. The adhesive demonstrates excellent chemical resistance and can withstand temperatures up to 140 °C, making it particularly suitable for applications requiring high mechanical performance under thermal stress. This adhesive is appropriate for industrial applications exposed to aggressive environments and elevated temperatures and can bond a variety of materials, including metals, ceramics, glass, rubbers, and rigid plastics. The shear strength in single lap joints with metallic substrates is between 15 and 20 MPa (manufacturer's data).

Araldite® 420 A/B is a two-component, dark green epoxy adhesive after mixing. It cures at room temperature and exhibits high shear and peel strength as well as excellent toughness. The adhesive also demonstrates good resistance to moisture and is suitable for bonding metals, composites, and honeycomb structures. It can bond a wide variety of substrates, including metals, wood, rubber, glass-fibre-reinforced polymers (GFRP), and many

plastics. The shear strength in single lap joints with metallic substrates is between 20 and 28 MPa (manufacturer's data). At room temperature, full curing is achieved within one to two weeks.

SikaForce® 710 L100 is a two-component polyurethane adhesive, comprising Component A (SikaForce® 710 L100, a polyol mixture) and Component B (SikaForce® 010, an isocyanate derivative mixture). Upon mixing, the adhesive exhibits a beige colour and cures at room temperature. It is primarily used for bonding metals, fibre cement, wood, and glass fibre to polystyrene foams, polyurethane foams, and mineral wool, making it suitable for the manufacture of sandwich panels and other construction applications.

Table 1 presents some properties of the three adhesives (manufacturer's data). The selected adhesives represent structurally distinct mechanical behaviours: a high-stiffness brittle epoxy (AV 138), a toughened epoxy with balanced strength and ductility (420 A/B), and a flexible polyurethane adhesive (SikaForce® 710). This contrast enables evaluation of the developed testing fixtures across a broad spectrum of stiffness, ductility, and failure mechanisms, thereby strengthening the validation of their versatility and robustness.

Table 1. Properties of the adhesives.

	Araldite® AV 138	**Araldite® 420 A/B**	**SikaForce® 710**
Young's modulus (GPa) (ISO 527 [44])	4.2	1.49	0.33 [45]
Tensile strength (MPa) (ISO 527 [44])	29	29	14
Elongation at break (%) (ISO 527 [44])	0.8	4.6	25
Lap shear strength (MPa) (ISO 4587 [46])	15–20	20–28	9
Shore Hardness	D86	D75	D72
Viscosity @ 25 °C (Pa.s)	Thixotropic	35–45	10

2.3. Specimens Manufacturing for the Floating Roller Peel Test

According to ASTM D 3167 standard [38], the rigid and flexible substrates should have a width (b) of 12.7 mm and lengths (L) of 203.2 mm and 254 mm, respectively. If not otherwise specified, the standard recommends t_S = 1.63 mm for the rigid and t_S = 0.63 mm for the flexible substrates. In the present study, however, substrates with the nominal dimensions listed in Table 2 were used.

The nominal adhesive bondline thickness was set to 0.2 mm. Although manufacturer datasheets for Araldite® AV 138 and Araldite® 420 A/B recommend a range of 0.05–0.10 mm, a thickness of 0.2 mm was adopted, as this value is commonly reported in the literature for structural adhesive characterisation, ensuring comparability with previously reported peel studies [31,32] and minimizing bending-induced artefacts that may affect peel strength measurements. Furthermore, it provides improved tolerance to minor surface irregularities while promoting uniform stress distribution. The same thickness was maintained for SikaForce® 710 to avoid introducing bondline thickness as a variable. Thickness control was achieved using calibrated 0.20 mm copper wires positioned at the overlap extremities and left in place, without affecting the analysed steady-state peel region.

Table 2. Nominal dimensions of substrates employed in the floating roller peel test.

Adherend	**L (mm)**	**b (mm)**	**t_S (mm)**
Rigid	200	20	3.0
Flexible	250	20	0.50

First, the surface of the Al-alloy AW 6082-T6 substrates intended for adhesive application was prepared using two passive treatments: a mechanical and a chemical one. The substrates were abraded with sandpaper or grit blasted and then wiped clean with an acetone-soaked cloth. The selection of abrasion and grit blasting was based on their widespread use in structural adhesive bonding and their documented influence on surface roughness and mechanical interlocking [22,33]. Abrasion provides moderate surface activation, whereas grit blasting generates increased surface roughness and enhanced mechanical anchoring. The use of both methods enables evaluation of adhesive sensitivity to surface morphology and interfacial adhesion mechanisms.

The grit blasting was performed on both sides of the substrates to minimize deformation caused by the stresses introduced by this surface treatment. During the bonding of the substrates, the adhesive layer was applied to the treated area of the rigid substrate, covering approximately 150 mm, and was bounded by two regions of approximately 40 mm and 10 mm without adhesive. These adhesive-free regions serve to calibrate the adhesive

thickness (t_A). Within each interior edge adjacent to the adhesive layer, two copper wires with a diameter of 0.20 mm were positioned to control the thickness of the adhesive film. The ≈40 mm adhesive-free length allows the rigid substrate to rest on both rollers, thereby facilitating the initiation of the peel process during testing. According to the test standard, this length should range between 38.1 mm and 74.2 mm. The configuration of the joint is illustrated in Figures 4 and 5 shows some manufactured joints.

Surface preparation was conducted under controlled conditions to ensure consistency between specimens. Abrasion was performed using P500 grit sandpaper with uniform manual pressure along a single direction (abrading in the longitudinal direction, that is, in the direction of the substrate length). Grit blasting was carried out using identical process parameters for all specimens, including consistent exposure time and nozzle distance. After treatment, substrates were cleaned with acetone to remove debris and contaminants. The Arithmetic Average Roughness (R_a) was measured with Mahr M2 Perthometer, and for substrates with AW 6082-T6 alloy, the roughness obtained by abrading was R_a = 0.46 µm (standard deviation = ±0.05) and by grit blasting was R_a = 5.20 µm (STD = ±0.38). For substrates with AW 1050 alloy, the roughness obtained by abrading was R_a = 0.91 µm (STD = ±0.11) and by grit blasting was R_a= 5.66 µm (STD = ±0.60). The roughness for the AW 1050 alloy is slightly higher because this alloy has a lower hardness than the AW 6082-T6 alloy. Five repetitions were performed for each sample.

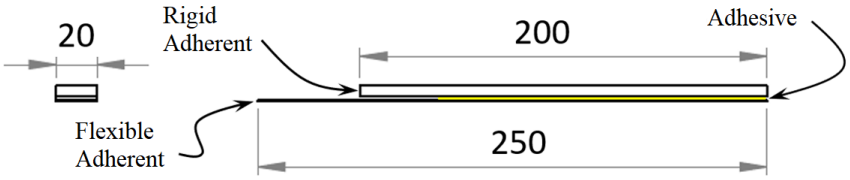

Figure 4. Geometry of the floating roller peel test specimens (dimensions in mm).

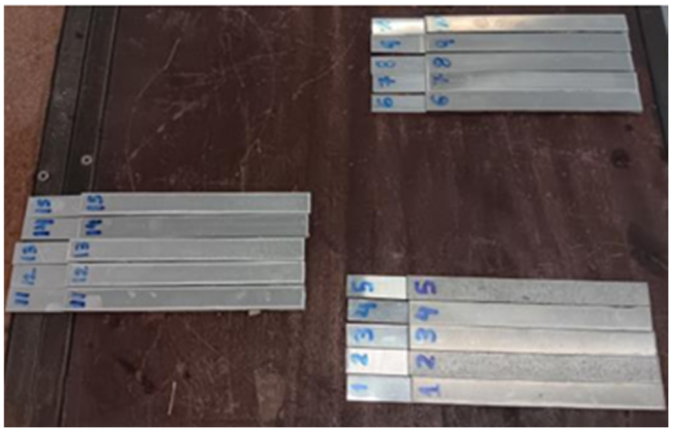

Figure 5. Some floating roller peel test specimens after removal of excess adhesive.

2.4. Specimens Manufacturing for the Butt-Joint Test

The butt-joint specimens were manufactured in accordance with the general recommendations of ASTM D 2094 standard [39], with controlled adaptations introduced to accommodate the custom-developed alignment fixture. The specimen geometry and nominal dimensions are illustrated in Figure 6. All substrates were machined to the specified dimensions using standard machining practices, and dimensional verification was performed using digital callipers prior to bonding to ensure geometric consistency and compliance with nominal tolerances.

Surface preparation was conducted to promote interfacial adhesion and ensure repeatability across all specimens. The preparation procedure consisted of (1) Cleaning with acetone to remove oils and surface contaminants; (2) Mechanical abrasion of the bonding surface using P500 grit sandpaper applied uniformly along a single direction; (3) Cleaning with compressed air to remove abrasive debris, and (4) Final cleaning with acetone to ensure a contaminant-free surface prior to bonding. All substrates were prepared using identical procedures to minimise variability in surface condition between specimens and adhesive types.

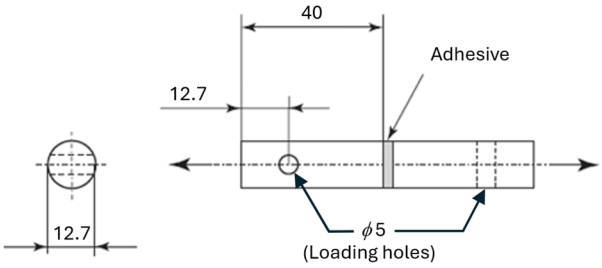

Figure 6. Butt-joint geometry (dimensions in mm).

The fabrication of the butt joints began with the preparation of the bonding surfaces of the substrates. These substrates are reusable after the removal of residual adhesive following testing. The surface preparation procedure consisted on: (1) cleaning with acetone to remove oils and lubricants, (2) abrading the bonding surface with P500 grit sandpaper, (3) cleaning with compressed air, followed by a second cleaning with acetone. The surface roughness was measured with Mahr M2 Perthometer, and the roughness obtained was R_a = 0.51 μm (standard deviation = ±0.05). Five repetitions were performed for each sample.

After surface preparation, the joints were fabricated using a custom fixture apparatus developed and manufactured in-house (Figure 7). This apparatus ensures proper alignment of the substrates and the desired thickness for the adhesive, which in this case was 0.2 mm. The adhesive thickness of 0.2 mm was selected to represent typical structural bonding conditions reported in the literature [12,36], while minimizing stress concentrations associated with excessively thick adhesive layers. Accurate thickness control is essential to ensure repeatability and reliable stress distribution during tensile loading. Measurements were performed in three equally spaced angular positions (≈120° apart), confirming a thickness close to the nominal value.

Adhesive curing was carried out at room temperature, for the same period conducted for each adhesive, in the floating roller peel specimens. Figure 8 depict the fabricated butt joints prepared for tensile testing. The excess adhesive was removed after curing using files and abrasive papers to ensure a clean and uniform finish. On a short note, six specimens were fabricated with Araldite® AV 138; however, only five were tested under tensile loading conditions.

All specimens were machined to the specified nominal dimensions with standard machining tolerances. Dimensional verification was performed using digital calipers prior to bonding to ensure consistency with ASTM standard requirements.

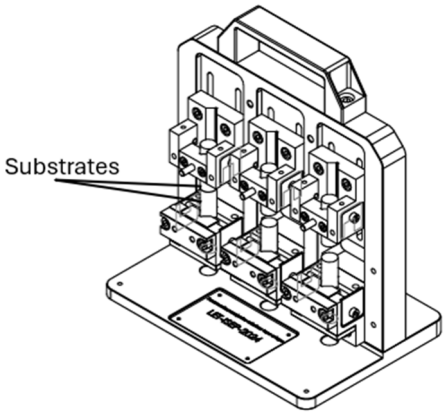

Figure 7. Apparatus for manufacturing butt-joints.

Figure 8. Butt joints after removal of excess adhesive (**a**) Araldite® AV 138, (**b**) Araldite® 420 A/B and (**c**) SikaForce® 710 L100.

Microscopic analysis was performed with the microscope depicted in Figure 9. Afterwards, using the NIS-ELEMENTS software, it confirmed that the adhesive layer was uniform and its thickness closely matched the target value of 0.2 mm, as illustrated from Figures 10–12. The adhesive thickness was measured in three distinct regions, each offset by approximately 120°.

Figure 9. Microscope Olympus SZ1145TR.

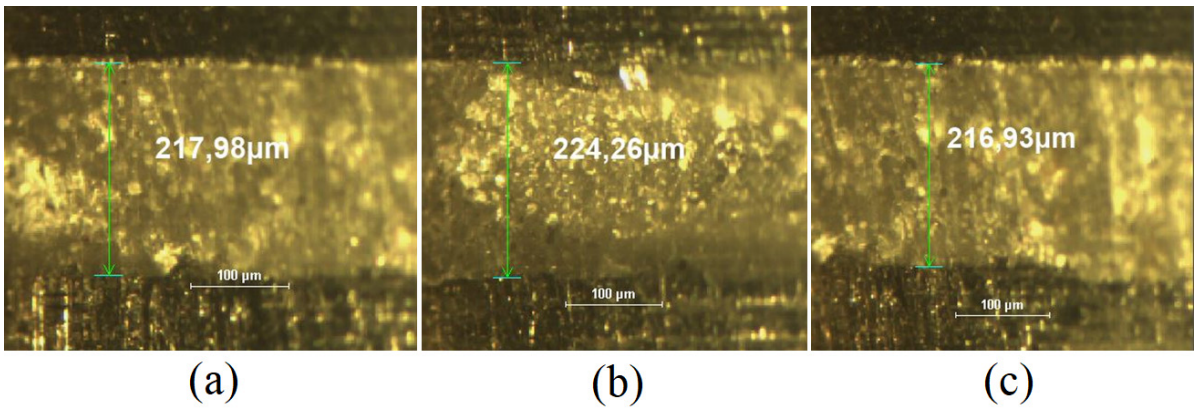

Figure 10. Adhesive thickness—Araldite® AV 138 (**a**), measurement at 0° specimen rotation, (**b**) measurement at 120° specimen rotation, (**c**) measurement at 240° specimen rotation.

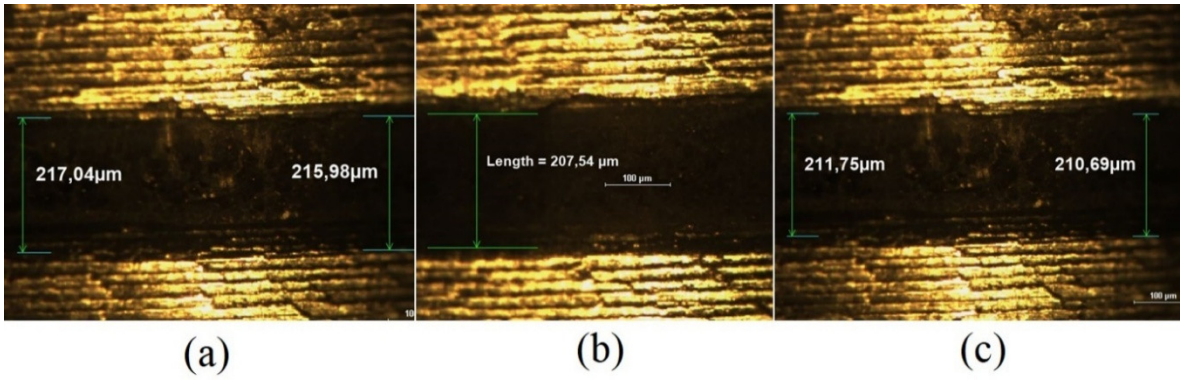

Figure 11. Adhesive thickness—Araldite® 420 A/B, (**a**) measurement at 0° specimen rotation, (**b**) measurement at 120° specimen rotation, (**c**) measurement at 240° specimen rotation.

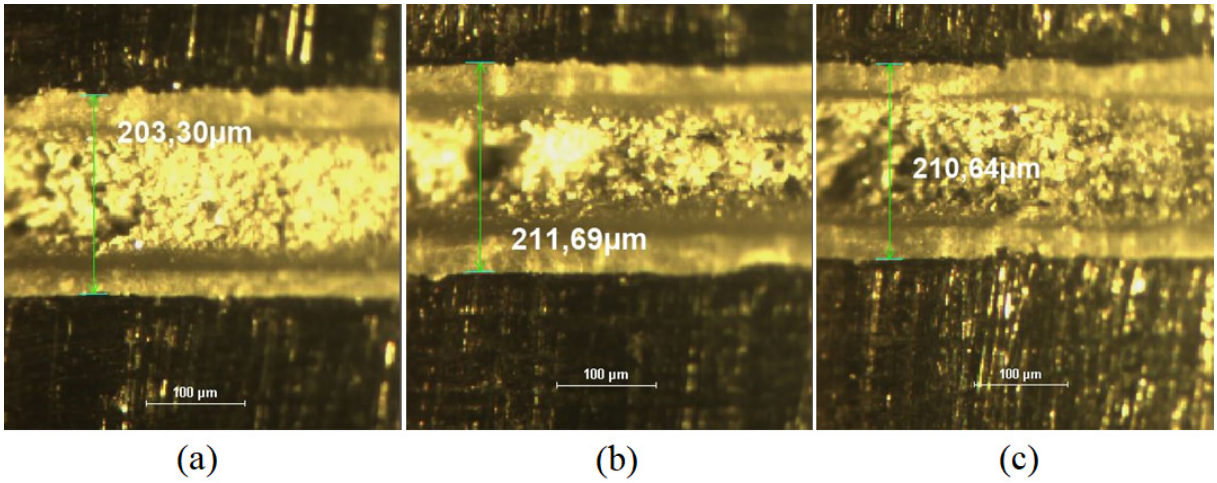

Figure 12. Adhesive thickness—SikaForce® 710 L100, (**a**) measurement at 0° specimen rotation, (**b**) measurement at 120° specimen rotation, (**c**) measurement at 240° specimen rotation.

Prior to testing, all specimens (for the floating roller and for the tensile tests) were visually inspected for bonding defects, voids, or misalignment. Only specimens exhibiting uniform adhesive distribution and proper curing were selected for mechanical testing.

2.5. Test Procedure for the Floating Roller Test

The floating roller peel tests were conducted, according to ASTM D 3167 standard [38], at room temperature, with a test speed of 152 mm/min and an initial preload of 5 N, using a Shimadzu AG-I 10 kN tensile testing machine, as shown in Figure 13. The selected crosshead speed follows the ASTM D 3167 standard [38], ensuring controlled strain-rate conditions and consistency with previously reported adhesive peel characterisation studies [31].

Figure 13. Shimadzu AG-I 10 kN tensile testing machine with a floating roller test apparatus installed.

A 5 kN load cell with a working range limited to 500 N was employed to enhance the sensitivity of the recorded load (P) evolution. During the tests, the system continuously recorded both the applied load and the displacement (δ) of the machine's upper crosshead. All tests were performed two weeks after joint fabrication and five tests were performed for each condition. Figure 14 show the floating roller fixture employed in this study and illustrates a joint mounted on the device, with the flexible adherend clamped in the machine's lower jaw and the rigid adherend positioned on the rollers. This floating roller device was developed and manufactured in-house, and the peel tests performed in this work aim to characterize the adhesives and the performance of this device.

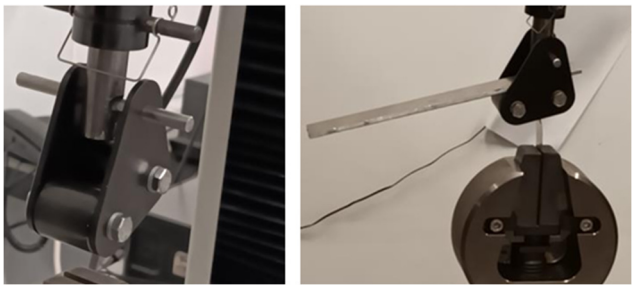

Figure 14. Floating roller test apparatus manufactured in-house without specimen (**left**) and with test specimen (**right**) installed in the tensile machine.

2.6. Test Procedure for the Butt-Joints Tensile Test

The butt-joint tests were performed in accordance with ASTM D 2095 standard [40], at room temperature, with a test speed of 0.5 mm/min and an initial preload of 5 N, using a Shimadzu AG-I 10 kN testing machine equipped with a 10 kN load cell, as shown in Figure 15. This displacement rate complies with ASTM D 2095 standard [40] and is commonly adopted in tensile characterisation of structural adhesives to minimise dynamic effects and ensure quasi-static loading conditions [36].

To correct the axial alignment during the test, a device with a cardan was connected to the test machine. This device was developed and manufactured in-house. The specimens were tested two weeks after joint fabrication, and five tests were performed for each adhesive. The stress is obtained by dividing the load by the loaded area.

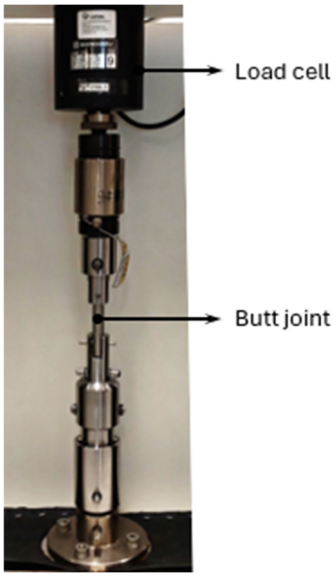

Figure 15. Shimadzu AG-I 10 kN tensile testing machine with a tensile test apparatus installed for butt joints.

3. Results and Discussion

3.1. Floating Roller Peel Test

According to the applicable testing standards, the key parameters to consider are the average load (P_{ave}), maximum load (P_{max}), and minimum load (P_{min}). These values should be determined over a δ of at least 75 mm, disregarding the initial 25 mm of δ. From these values, the parameters P_{ave}/b, P_{max}/b, and P_{min}/b are calculated. The parameter (b) corresponds to the specimen width. Another critical outcome is the type of joint failure observed. It should be noted that tests were carried out with substrates prepared by abrading and grit blasting. The peel strength (P/b) ± standard deviation and failure type are given in Table 3. The reported results are the average values obtained from five specimens for each adhesive. The P/b—δ curves for substrates prepared by abrading and substrates prepared by grit blasting are shown in Figures 16 and 17, respectively.

Table 3. Peel strength and failure mode.

	Adhesive	P_{ave}/b (N/mm)	P_{max}/b (N/mm)	P_{min}/b (N/mm)	Type of Failure
Abrading	AV 138	0.32 ± 0.08	0.47 ± 0.05	0.25 ± 0.08	Mainly adhesive
	420 A/B	2.55 ± 0.65	3.03 ± 0.65	1.92 ± 0.75	Mainly adhesive
	SKF 710	4.44 ± 0.38	5.14 ± 0.59	3.61 ± 0.33	3 adhesive and 2 mixed
Grit blasting	AV 138	1.35 ± 0.37	1.86 ± 0.48	1.01 ± 0.23	Mainly cohesive
	420 A/B	5.24 ± 0.59	6.03 ± 0.37	4.67 ± 0.63	Mainly adhesive
	SKF 710	5.41 ± 0.30	6.16 ± 0.43	4.75 ± 0.26	Mixed

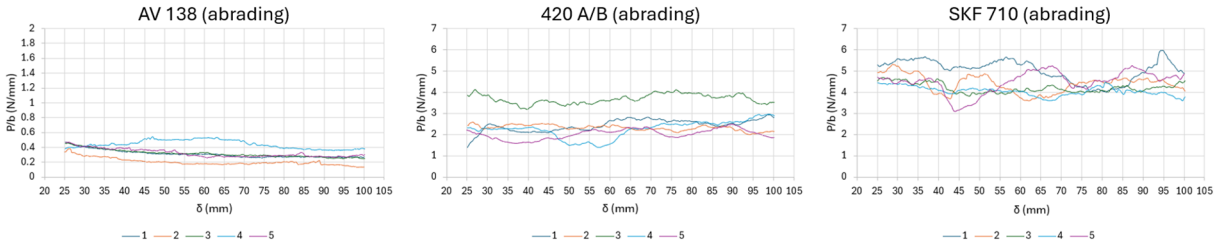

Figure 16. Peel load versus displacement curves for substrates prepared by abrading.

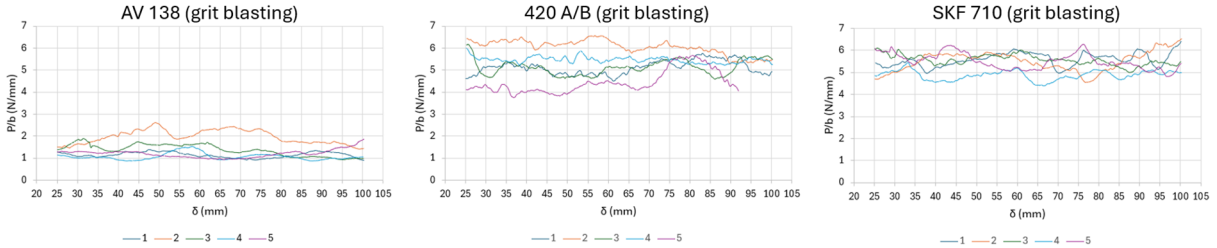

Figure 17. Peel load versus displacement curves for substrates prepared by grit blasting.

In Figure 16, the graph for the AV 138 adhesive (abrading) has a different scale on the y-axis due to the very low P/b values. All other graphs have the same scale for easier comparison.

From the results presented, it is easy to observe that, regardless of the surface preparation method, adhesive AV 138 exhibited the lowest peel strength, confirming its markedly brittle behaviour. For sandpaper abrasion, the peel strength (P_{ave}/b) of this adhesive was only 0.32 ± 0.08 N/mm, while for grit blasting it increased to 1.35 ± 0.37 N/mm. Conversely, adhesive SKF 710, which is a ductile and flexible adhesive, showed the highest peel strength. For sandpaper abrasion, its peel strength was 4.44 ± 0.38 N/mm, while for grit blasting it reached 5.41 ± 0.30 N/mm. Adhesive 420 A/B, which combines high strength with excellent toughness, exhibited significantly higher peel strength than AV 138 and, when grit blasting was used, achieved peel strength values close to those obtained with SKF 710. For sandpaper abrasion, its peel strength was 2.55 ± 0.65 N/mm, increasing considerably to 5.24 ± 0.59 N/mm with grit blasting. These trends are also evident in Figure 18, which compares peel strength for the three adhesives and both surface preparation methods.

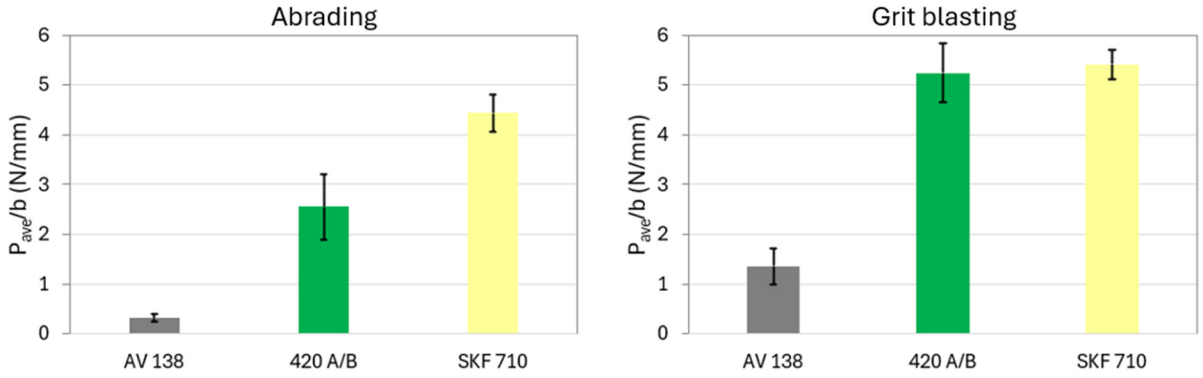

Figure 18. Peel strength and standard deviations versus adhesive type and surface preparation.

The fracture surfaces are shown in Figures 19 and 20. Three types of failure mechanisms were observed: adhesive failure at the interface between the adhesive and adherend, cohesive failure within the adhesive and mixed failure, which presents areas with characteristics of adhesive failure and areas with characteristics of cohesive failure. The adhesive failure indicates a bad adhesion between the adhesive and the adherend and prevents the adhesive from reaching its full potential. Cohesive failure indicates good adhesion, since the failure is within the adhesive layer and not at the interface. Mixed failure is usually associated with inadequate surface preparation. Mixed failure can be classified as mainly adhesive or mainly cohesive. In the first case, the area of the fracture surface with characteristics of an adhesive failure is more predominant. In the second case, the area of the fracture surface with characteristics of a cohesive failure is more predominant. It should be noted that in this study, the classification of the type of failure was performed by visual inspection.

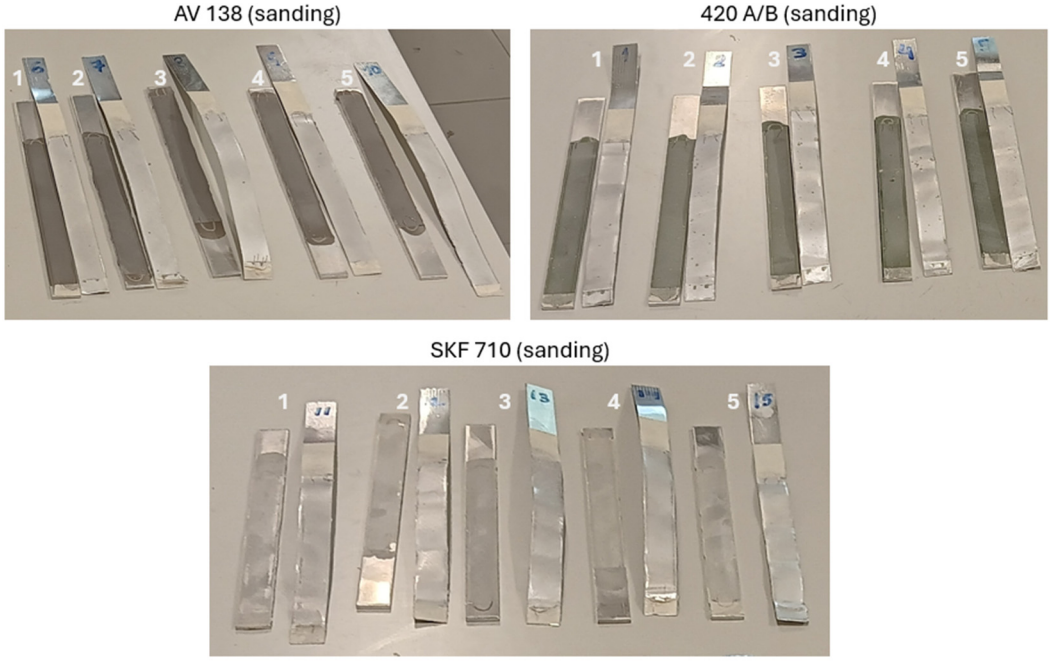

Figure 19. Failure surfaces of substrates prepared by abrading.

Grit blasting increased the peel strength for all three adhesives, with a more pronounced effect observed for the epoxy adhesives (AV 138 and 420 A/B). This indicates that grit blasting enhances mechanical interlocking between the adhesive and the substrate surface. With sandpaper abrasion, failure was generally adhesive, with the adhesive layer remaining mostly on the rigid substrate. In contrast, grit blasting led, in several cases, to cohesive or mixed failure modes. For AV 138, although grit blasting promoted predominantly cohesive failure near the flexible substrate interface, peel strength remained relatively low due to the intrinsic brittleness of the adhesive. For adhesive 420 A/B, failure was predominantly adhesive regardless of surface preparation; however, grit blasting significantly increased peel strength by improving anchoring at the substrate surface, even though the interface remained the weakest link. For SKF 710, peel strength also increased with grit blasting, although to a lesser extent, indicating that this adhesive is less sensitive to surface preparation. Overall, epoxy adhesives (AV 138 and 420 A/B) were found to be more sensitive to surface treatment than the polyurethane adhesive SKF 710. Failure was predominantly adhesive, particularly for specimens prepared by abrasion.

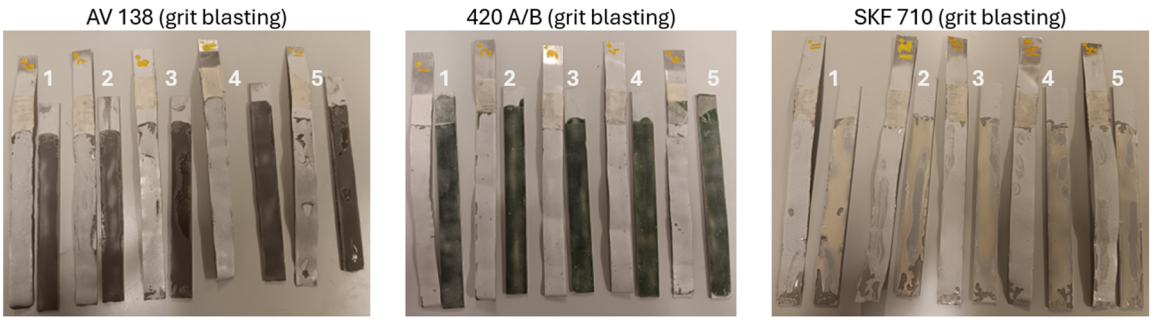

Figure 20. Failure surfaces of substrates prepared by grit blasting.

Comparing the results obtained in this work with those reported in the work carried out by Pereira et al. [47], it is possible to verify that the results are identical. In the work developed by these authors, AV 138 adhesive and aluminium and composite substrates were used. For the floating roller peel tests with aluminium substrates prepared by surface abrasion with sandpaper and then wiping clean with an acetone-soaked cloth, the peel strength was also quite low (P_{ave}/b = 0.375 N/mm) and the type of failure was also adhesive. de Freitas and Sinke [48] performed floating roller peel tests with the epoxy film adhesives FM 73 (Cytec Eng. Mat.) and EA 9695 (Henkel). In this work, the peel strength with aluminium adherends was 11 N/mm for FM 73 and 2.08 N/mm for EA 9695. The peel strength of AV 138 is lower since it is a brittle adhesive, while FM 73 and EA 9695 are flexible toughened adhesives developed for the aerospace industry. In another study from de Freitas and Sinke [49], where peel strength of nine adhesives in specimens with carbon fibre reinforced polymer and aluminium adherends was compared, the results obtained for the aluminium specimens ranged from 0.60 N/mm to 11.88 N/mm. This shows that the peel strength obtained in this work for the AV 138, 420 A/B and SKF 710 adhesives is within the values indicated in the literature.

3.2. Butt-Joint Test

The butt-joint tests were primarily conducted to validate the performance of each adhesive to tensile loads. The average values and standard deviation from the tensile tests of the butt joints are presented in Table 4. This table also displays the failure modes obtained for the three adhesives. The reported results are the average values obtained from five specimens for each adhesive. Surface preparation involved abrasion with sandpaper and then wiping clean with an acetone-soaked cloth.

Table 4. Tensile strength and failure mechanisms for butt-joints specimens.

Adhesive	P_{max} (N/mm)	σ_{max} (MPa)	δ_{max} (mm)	Type of Failure
AV 138	3678.56 ± 133.23	29.04 ± 1.05	0.72 ± 0.03	Cohesive
420 A/B	2626.13 ± 258.15	20.73 ± 2.04	0.52 ± 0.05	1 Cohesive/2 Adhesive/2 Mixed
SKF 710	1081.88 ± 91.68	8.54 ± 0.72	0.31 ± 0.03	Cohesive

In Figure 21 are shown the P–δ curves for each butt-joint specimen. However, the tensile strength of the three adhesives can be more easily compared using the graph in Figure 22, which shows the maximum tensile strength and the respective standard deviations for each adhesive. As depicted in the graphs, the AV 138 displays the most mechanical performance from the three adhesives, followed by the 420 A/B and SikaForce® 710. The Araldite® AV 138 showed the highest tensile strength (29.04 MPa) and SikaForce® 710 showed the lowest tensile strength (8.54 MPa). The tensile strength of Araldite® 420 A/B (20.73 MPa) was lower than that of AV 138 but much higher than that of SKF 710.

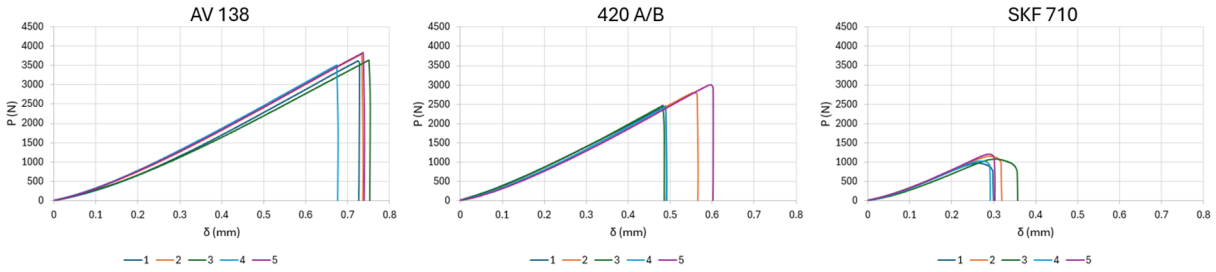

Figure 21. Tensile load versus displacement curves for the three adhesives.

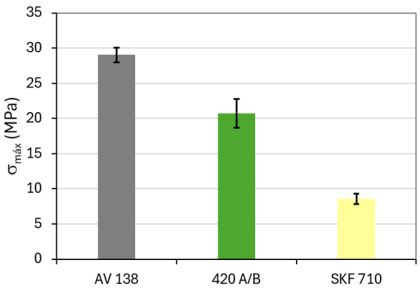

Figure 22. Tensile strength among the different adhesives.

The fracture surfaces are shown in Figure 23. The predominant failure mechanism was cohesive failure, indicating a good adhesion between the adhesives and the adherends (AISI 304 steel). For this reason, unlike peel tests, surface preparation by grit blasting was not used in these butt tension tests. Only three specimens with 420 A/B adhesive did not exhibit cohesive failure, suggesting that the surfaces of the adherends in these specimens may not have been adequately prepared or that the preparation method may require modification. The different failure modes observed with the 420 A/B adhesive contributed to the higher standard deviation observed in the results obtained with this adhesive.

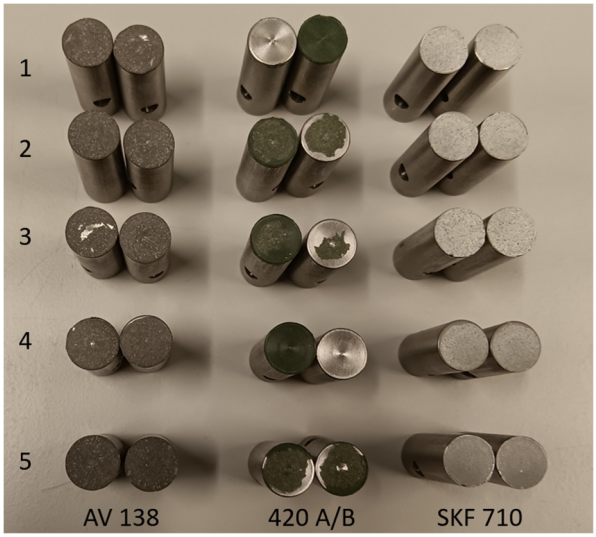

Figure 23. Failure surfaces of butt-joint specimens for the three adhesives.

Comparing the tensile strength values obtained in this work with those indicated by the manufacturers (see Table 1), it is possible to verify that for the AV 138 adhesive the values are identical, but for the 420 A/B and SKF 710 adhesives there is a certain difference. For the AV 138 adhesive, the measured joint strength (29.04 MPa) closely matches the tensile strength reported by the manufacturer (29 MPa). For the 420 A/B adhesive, the measured joint strength (20.73 MPa) is approximately 29% lower than the manufacturer's reported value (29 MPa). As expected, the SKF 710 adhesive exhibited the lowest strength (8.54 MPa), being approximately 39% lower than indicated in the technical datasheet (14 MPa). Based on this comparison, it can be concluded that the difference is greater for the more ductile adhesives. The difference observed for adhesive 420 A/B is also due to two specimens with adhesive failures that contributed to a decrease in the average tensile strength value obtained in the tests carried out in this work. Another factor contributing to the difference indicated above is that the tensile strength shown in Table 1 was obtained with bulk adhesive specimens according to ISO 524. In this work, however, the tensile strength was obtained with tensile tests of butt joints and, therefore, with thin adhesive layers. In tensile testing of butt joints, the lateral contraction of the adhesive does not occur freely, which introduces additional radial and circumferential stresses, especially at the edges of the joint. In addition to the constraining effect of the substrate, misalignments can occur during fabrication or testing, which introduce bending in the adhesive [50]. These factors prevent a direct comparison between the adhesive bulk properties and the measured properties with the adhesive in a thin layer between two steel substrates as in the butt joint. However, the tensile test of butt joints, when compared with tensile tests with bulk specimens, also presents several advantages: it requires less adhesive, the manufacture of samples is easier, the adherends are reusable, and it allows studying the effect of the surface preparation of the substrates.

4. Conclusions

This study reports the experimental validation of in-house manufactured devices designed for floating roller peel tests and tensile butt-joint tests, with the objective of enabling reliable mechanical characterization of structural adhesives. The effectiveness of the developed fixtures was assessed using three commercially relevant adhesives: two epoxy adhesives (Araldite® AV 138 and Araldite® 420 A/B) and one polyurethane adhesive (SikaForce® 710).

A total of thirty floating roller peel tests were performed on aluminium alloy substrates prepared using two different surface treatment methods, namely abrading and grit blasting. In addition, fifteen tensile butt-joint tests were conducted on stainless steel substrates. The experimental work demonstrated the robustness, repeatability,

and suitability of the developed fixtures for adhesive characterisation over a broad range of mechanical behaviours. The device used for the floating roller tests kept the specimen properly aligned on the rollers, which rotated in accordance with the adherend displacement, thereby preventing friction between the adherends and the roller surfaces. The tooling used for the manufacture of the butt joints enabled proper axial alignment of the adherends and ensured the desired thickness of the adhesive layer. The fixture used to subject the butt joint to tensile loading ensured correct alignment of the specimen with the load application direction, thereby preventing the introduction of additional loading modes, such as bending or torsion.

The results obtained from the floating roller peel tests allow the following conclusions to be drawn:

- Araldite® AV 138 showed the lowest peel strength, with values of 1.35 N/mm for grit-blasted surfaces and only 0.32 N/mm for abraded surfaces, consistent with its brittle mechanical behaviour.
- Araldite® 420 A/B demonstrated good peel performance, particularly for grit-blasted substrates (5.24 N/mm), approaching the values obtained with SikaForce® 710, while remaining clearly superior to Araldite® AV 138. For abraded surfaces the peel strength was 2.55 N/mm.
- SikaForce® 710 exhibited the highest peel strength, reaching 5.41 N/mm for grit-blasted surfaces and 4.44 N/mm for abraded surfaces, reflecting its high ductility and flexibility.
- In all cases, grit blasting significantly enhanced peel strength, especially for epoxy adhesives, confirming the critical role of mechanical interlocking and surface roughness in improving joint performance.
- The observed failure modes indicate a shift from predominantly adhesive failure in abraded surfaces to cohesive or mixed failure in grit-blasted surfaces.

From the tensile butt-joint tests, the following conclusions were obtained:

- Araldite® AV 138 exhibited the highest tensile strength (29.04 MPa), closely matching manufacturer-reported values and confirming its high strength.
- Araldite® 420 A/B showed intermediate tensile strength (20.73 MPa), lower than AV 138 but significantly higher than SikaForce® 710. For this adhesive, in contrast to the other adhesives, the failure mode was not consistently cohesive.
- SikaForce® 710 presented the lowest tensile strength (8.54 MPa), consistent with its ductile nature and lower bulk strength.
- Predominantly cohesive failure modes were observed, indicating good adhesion between the adhesives and the steel substrates and validating the effectiveness of the adopted surface preparation method. The predominance of cohesive failure in the butt-joint tensile tests indicates that the adhesive–substrate interface exhibited higher strength than the bulk adhesive under normal tensile loading. In structural applications, however, adhesive joints are frequently subjected to combined normal and shear stresses. Previous studies have demonstrated that shear strength and tensile strength do not necessarily scale proportionally, as shear performance is strongly influenced by adhesive ductility, plastic deformation capability, and stress redistribution mechanisms [36,50]. While shear lap-joint testing could provide complementary insight into interfacial performance under tangential loading, the present study focuses on peel and normal tensile configurations to evaluate the robustness and alignment accuracy of the developed fixtures. The consistent cohesive failure observed suggests that the interface preparation was effective, and that the measured tensile strength primarily reflects intrinsic adhesive properties. Future investigations may incorporate shear-dominated configurations to further explore the relationship between normal and shear strength in these adhesive systems.
- The tensile butt-joint tests revealed a contrasting ranking of adhesive performance, governed primarily by intrinsic tensile strength rather than ductility.

Overall, the developed testing tools demonstrated effective and reliable performance for evaluating adhesive behaviour under both peel and tensile loading conditions. The results underscore the significant influence of adhesive mechanical properties and surface preparation on joint performance, and provide valuable experimental data to support adhesive selection, joint design, and quality control processes in structural engineering applications.

5. Future Work

Regarding future research, the following directions are proposed:

- Fabrication of butt joints cured at different temperatures (40, 80, 100, and 120 °C), in order to analyse the effect of curing temperature on the performance and dimensional stability of the tool developed for joint fabrication.
- Production of butt joints using substrates with other geometries and dimensions, since the current tool has only been validated for substrates of 12.7 mm in diameter and 40 mm in length. This would allow evaluation

of the tool's adaptability and assessment of the potential influence of geometric parameters on joint mechanical performance.

- Manufacture of butt joints using alternative adhesives and varying adhesive layer thicknesses, as the current tooling configuration has been validated only for adhesive layers with a thickness of 0.2 mm. This would enable analysis of thickness-dependent stress distribution and failure behaviour.
- Execution of additional floating roller peel tests using alternative adhesives and substrate materials, to broaden the comparative database and assess the versatility of the developed tool across different material–adhesive systems.
- Performance of shear-dominated mechanical tests (e.g., lap shear configurations) in cases where tensile testing demonstrates cohesive adhesive failure, to investigate potential relationships between ultimate shear strength and normal tensile strength. Such investigation may enable assessment of whether failure criteria based on equivalent stress approaches (e.g., von Mises or Tresca) can describe adhesive behaviour within restricted regimes (e.g., same adhesive family and controlled stress states).
- Conduct peel tests under quasi-constant loading or controlled steady-state peeling conditions, combined with tensile and shear characterisation, to explore whether restricted correlations between peel resistance and intrinsic adhesive strength can be established under fully cohesive failure and well-defined stress states.

Author Contributions

Conceptualisation: A.G.P. and P.J.R.O.N.; methodology: R.D.S.G.C. and A.G.P.; validation: R.D.S.G.C. and P.J.R.O.N.; formal analysis: A.F.V.P.; investigation: J.G.F.B. and D.A.M.S.; data curation: A.F.V.P. and A.G.P.; writing—original draft preparation: A.F.V.P., J.G.F.B. and D.A.M.S.; writing—review and editing: A.F.V.P., R.D.S.G.C. and A.G.P.; visualisation: R.D.S.G.C.; supervision: A.G.P. and P.J.R.O.N.; project administration: A.G.P. All authors have read and agreed to the published version of the manuscript.

Funding

This research received no external funding.

Data Availability Statement

Not applicable.

Conflicts of Interest

The authors declare that they have no competing interests

Use of AI and AI-Assisted Technologies

No AI tools were utilized for this paper.

References

1. Dachev, D.; Kazilas, M.; Alfano, G.; et al. Towards Reliable Adhesive Bonding: A Comprehensive Review of Mechanisms, Defects, and Design Considerations. *Materials* **2025**, *18*, 2724. https://doi.org/10.3390/ma18122724.
2. Demiral, M.; Mamedov, A. Comparison of the strength of resistance spot-welded, bonded, and hybrid single lap joints: A numerical investigation. *Results Eng.* **2025**, *25*, 103871. https://doi.org/10.1016/j.rineng.2024.103871.
3. Nonnenmann, T.; Beygi, R.; Carbas, R.J.C.; et al. Synergetic effect of adhesive bonding and welding on fracture load in hybrid joints. *J. Adv. Join. Process.* **2022**, *6*, 100122. https://doi.org/10.1016/j.jajp.2022.100122.
4. Wei, Y.; Jin, X.; Luo, Q.; et al. Adhesively bonded joints—A review on design, manufacturing, experiments, modeling and challenges. *Compos. Part B Eng.* **2024**, *276*, 111225. https://doi.org/10.1016/j.compositesb.2024.111225.
5. Delzendehrooy, F.; Akhavan-Safar, A.; Barbosa, A.Q.; et al. A comprehensive review on structural joining techniques in the marine industry. *Compos. Struct.* **2022**, *289*, 115490. https://doi.org/10.1016/j.compstruct.2022.115490.
6. Frascio, M.; Marques, E.A.d.S.; Carbas, R.J.C.; et al. Review of Tailoring Methods for Joints with Additively Manufactured Adherends and Adhesives. *Materials* **2020**, *13*, 3949.
7. Borges, C.S.P.; Akhavan-Safar, A.; Tsokanas, P.; et al. From fundamental concepts to recent developments in the adhesive bonding technology: A general view. *Discov. Mech. Eng.* **2023**, *2*, 8. https://doi.org/10.1007/s44245-023-00014-7.
8. Karthikeyan, N.; Naveen, J. Progress in adhesive-bonded composite joints: A comprehensive review. *J. Reinf. Plast. Compos.* **2025**, *44*, 1844–1890. https://doi.org/10.1177/07316844241248236.

9. Phiri, R.; Mavinkere Rangappa, S.; Siengchin, S.; et al. Advances in lightweight composite structures and manufacturing technologies: A comprehensive review. *Heliyon* **2024**, *10*, e39661. https://doi.org/10.1016/j.heliyon.2024.e39661.
10. Hassan, H.Z.; Saeed, N.M. Advancements and applications of lightweight structures: A comprehensive review. *Discov. Civ. Eng.* **2024**, *1*, 47. https://doi.org/10.1007/s44290-024-00049-z.
11. Galińska, A.; Galiński, C. Mechanical Joining of Fibre Reinforced Polymer Composites to Metals—A Review. Part II: Riveting, Clinching, Non-Adhesive Form-Locked Joints, Pin and Loop Joining. *Polymers* **2020**, *12*, 1681.
12. Ciardiello, R.; Boursier Niutta, C.; Goglio, L. Adhesive Thickness and Ageing Effects on the Mechanical Behaviour of Similar and Dissimilar Single Lap Joints Used in the Automotive Industry. *Processes* **2023**, *11*, 433.
13. Khan, F.; Hossain, N.; Mim, J.J.; et al. Advances of composite materials in automobile applications—A review. *J. Eng. Res.* **2025**, *13*, 1001–1023. https://doi.org/10.1016/j.jer.2024.02.017.
14. Zhang, W.; Xu, J. Advanced lightweight materials for Automobiles: A review. *Mater. Des.* **2022**, *221*, 110994. https://doi.org/10.1016/j.matdes.2022.110994.
15. Aparecida Silva, L.; Espinosa, C.; Chieragatti, R.; et al. Functionalization of Adhesive Bonding to Control On-Demand Disassembly of Composite Aeronautical Structures. *Aerospace* **2025**, *12*, 269.
16. Galib, G.; Silva, F.J.G.; Pedroso, A.F.V.; et al. A Comprehensive Review of Additive Manufacturing Technologies for Composite Materials. *J. Mech. Eng. Manuf.* **2025**, *1*, 2.
17. André, FV.P.; Rafael, L.; Luís, T.; et al. Electrical Discharge Machining of Composites: A Critical Review of Challenges and Innovations. *J. Mech. Eng. Manuf.* **2025**, *1*, 5. https://doi.org/10.53941/jmem.2025.100005.
18. Bañon, F.; Bermudo, C.; Trujillo, F.J.; et al. Adhesive Bonding Operations for Aeronautical Materials. In *Joining Operations for Aerospace Materials*; Gürgen, S., Ed.; Springer Nature: Cham, Switzerland, 2024; pp. 1–26.
19. Romano, M.G.; Guida, M.; Marulo, F.; et al. Characterization of Adhesives Bonding in Aircraft Structures. *Materials* **2020**, *13*, 4816.
20. Budzik, M.K.; Wolfahrt, M.; Reis, P.; et al. Testing mechanical performance of adhesively bonded composite joints in engineering applications: An overview. *J. Adhes.* **2022**, *98*, 2133–2209. https://doi.org/10.1080/00218464.2021.1953479.
21. Katsiropoulos, C.V.; Chamos, A.N.; Tserpes, K.I.; et al. Fracture toughness and shear behavior of composite bonded joints based on a novel aerospace adhesive. *Compos. Part B Eng.* **2012**, *43*, 240–248. https://doi.org/10.1016/j.compositesb.2011.07.010.
22. Yudhanto, A.; Alfano, M.; Lubineau, G. Surface preparation strategies in secondary bonded thermoset-based composite materials: A review. *Compos. Part A: Appl. Sci. Manuf.* **2021**, *147*, 106443. https://doi.org/10.1016/j.compositesa.2021.106443.
23. Cavezza, F.; Boehm, M.; Terryn, H.; et al. A Review on Adhesively Bonded Aluminium Joints in the Automotive Industry. *Metals* **2020**, *10*, 730.
24. Abdel-Monsef, S.; Renart, J.; Carreras, L.; et al. Environmental effects on the cohesive laws of the composite bonded joints. *Compos. Part A: Appl. Sci. Manuf.* **2022**, *155*, 106798. https://doi.org/10.1016/j.compositesa.2021.106798.
25. Demiral, M. Strength in Adhesion: A Multi-Mechanics Review Covering Tensile, Shear, Fracture, Fatigue, Creep, and Impact Behavior of Polymer Bonding in Composites. *Polymers* **2025**, *17*, 2600.
26. Jordan, A.; Hermelingmeier, L.; Gilich, J.; et al. Comparison of the economic efficiency and sustainability of two debonding processes for structurally bonded sills. *J. Adv. Join. Process.* **2025**, *12*, 100332. https://doi.org/10.1016/j.jajp.2025.100332.
27. Fan, C.; Chen, H.; Lin, F.; et al. Impact of Curing Time and Temperature on Bond Performance of Epoxy Resin Adhesives for Steel Bridge Decks. *Polymers* **2025**, *17*, 1018.
28. Andrady, A.L.; Heikkilä, A.M.; Pandey, K.K.; et al. Effects of UV radiation on natural and synthetic materials. *Photochem. Photobiol. Sci.* **2023**, *22*, 1177–1202. https://doi.org/10.1007/s43630-023-00377-6.
29. Venkatappagari, S.; Mutra, R.R.; Mallikarjuna Reddy, D. State-of-the-art in adhesive joint technology: A comprehensive review of recent progress. *J. Mater. Res. Technol.* **2025**, *37*, 2593–2615. https://doi.org/10.1016/j.jmrt.2025.06.166.
30. Alpendre, J.M.B.; Rosado, P.M.S.; Sampaio, R.F.V.; et al. Enhancing the performance of double-flush riveted joints through hybridization with adhesive bonding. *J. Adv. Join. Process.* **2025**, *12*, 100324. https://doi.org/10.1016/j.jajp.2025.100324.
31. Nóbrega, J.B.S.; Campilho, R.D.S.G.; Sánchez-Arce, I.J.; et al. Numerical estimation of the peel strength of adhesive joints via the floating roller peel test. *Procedia Struct. Integr.* **2023**, *47*, 408–416. https://doi.org/10.1016/j.prostr.2023.07.084.
32. Bartlett, M.D.; Case, S.W.; Kinloch, A.J.; et al. Peel tests for quantifying adhesion and toughness: A review. *Prog. Mater. Sci.* **2023**, *137*, 101086. https://doi.org/10.1016/j.pmatsci.2023.101086.
33. Pan, Y.; Wu, G.; Huang, Z.; et al. Effect of surface roughness on interlaminar peel and shear strength of CFRP/Mg laminates. *Int. J. Adhes. Adhes.* **2017**, *79*, 1–7. https://doi.org/10.1016/j.ijadhadh.2017.08.004.
34. Park, J.-H.; Oh, K.-H.; Oh, S.-K.; et al. A Study of the Field Test Method for the Adhesive Performance Evaluation of Self-Adhesive Waterproofing Sheets. *Appl. Sci.* **2023**, *13*, 8974.
35. Bahrami, M.; del Real, J.C.; Mehdikhani, M.; et al. Hybridization Effect on Interlaminar Bond Strength, Flexural Properties, and Hardness of Carbon–Flax Fiber Thermoplastic Bio-Composites. *Polymers* **2023**, *15*, 4619. https://doi.org/10.3390/polym15244619.

36. Öchsner, A.; Stasiek, M.; Mishuris, G.; et al. A new evaluation procedure for the butt-joint test of adhesive technology: Determination of the complete set of linear elastic constants. *Int. J. Adhes. Adhes.* **2007**, *27*, 703–711. https://doi.org/10.1016/j.ijadhadh.2006.12.003.
37. Raffa, M.L.; Rizzoni, R.; Lebon, F. A Model of Damage for Brittle and Ductile Adhesives in Glued Butt Joints. *Technologies* **2021**, *9*, 19.
38. *ASTM D 3167-10*; Standard Test Method for Floating Roller Peel Resistance of Adhesives. A. International: Philadelphia, PA, USA, 2010.
39. *ASTM D 2094-00*; Standard Practice for Preparation of Bar and Rod Specimens for Adhesion Tests. A. International: Philadelphia, PA, USA, 2014.
40. *ASTM D 2095-96*; Standard Test Method for Tensile Strength of Adhesives by Means of Bar and Rod Specimens. A. International: Philadelphia, PA, USA, 2015.
41. Zheng, R.; Lin, J.-P.; Wang, P.-C.; et al. Effect of hot-humid exposure on static strength of adhesive-bonded aluminum alloys. *Def. Technol.* **2015**, *11*, 220–228. https://doi.org/10.1016/j.dt.2015.01.005.
42. Witkowska, M.; Thompson, G.E.; Hashimoto, T.; et al. Assessment of the surface reactivity of AA1050 aluminium alloy. *Surf. Interface Anal.* **2013**, *45*, 1585–1589. https://doi.org/10.1002/sia.5271.
43. Sun, Y. The use of aluminum alloys in structures: Review and outlook. *Structures* **2023**, *57*, 105290. https://doi.org/10.1016/j.istruc.2023.105290.
44. *ISO 527-1:2012(E)*; Plastics-Determination of Tensile Properties-Part 1: General Principles. I. O. f. Standardization: Genebra, Suíça, 2012.
45. Sales, F.C.P.; Ariati, R.M.; Noronha, V.T.; et al. PU tensile tests: Conventional and digital image correlation analysis. *Procedia Struct. Integr.* **2022**, *37*, 389–396. https://doi.org/10.1016/j.prostr.2022.01.100.
46. *ISO 4587:2003(E)*; Adhesives—Determination of Tensile Lap-Shear Strength of Rigid-to-Rigid Bonded Assemblies, I. O. f. Standardization: Geneva, Switzerland, 2003.
47. Pereira, J.P.O.; Campilho, R.G.S.G.; Nóvoa, P.J.R.O.; et al. Adherend effect on the peel strength of a brittle adhesive. *Procedia Struct. Integr.* **2022**, *37*, 722–729. https://doi.org/10.1016/j.prostr.2022.02.002.
48. de Freitas, S.T.; Sinke, J. Adhesion Properties of Bonded Composite-to-Aluminium Joints Using Peel Tests. *J. Adhes.* **2014**, *90*, 511–525. https://doi.org/10.1080/00218464.2013.850424.
49. de Freitas, S.T.; Sinke, J. Test method to assess interface adhesion in composite bonding. *Appl. Adhes. Sci.* **2015**, *3*, 9. https://doi.org/10.1186/s40563-015-0033-5.
50. da Silva, L.F.M. Failure Strength Tests. In *Handbook of Adhesion Technology*; da Silva, L.F.M., Öchsner, A., Adams, R.D., Eds.; Springer: Berlin, Germany, 2011; pp. 443–471.